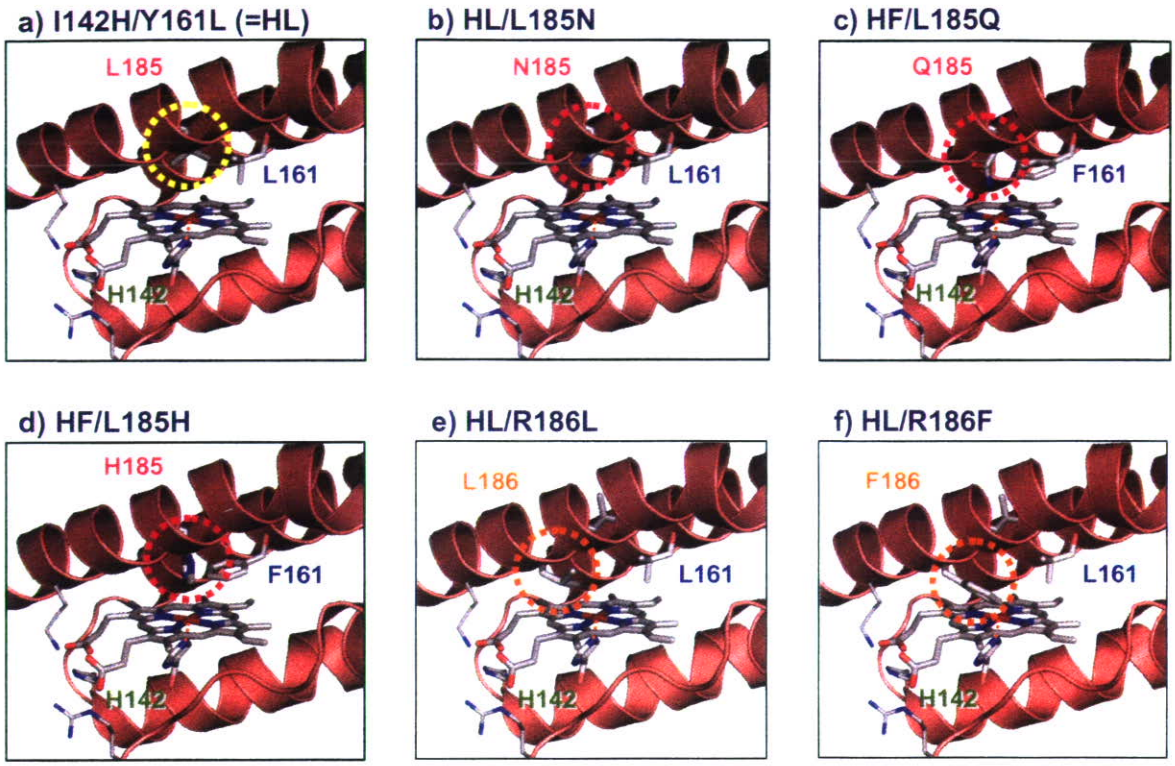

Figure 2. Structural models of the heme pocket in rHSA(mutant)–heme complexes.

O_2 Binding affinity of rHSA(HL)–heme

The rHSA(HL)–hemin was reduced to a ferrous complex by adding a small molar excess of aqueous sodium dithionate under an Ar atmosphere. A single broad absorption band (λ_{max}: 559 nm) in the visible region of rHSA(HL)–heme resembled that observed for deoxy Mb[13] or the chelated protoheme in DMF,[14] indicating the formation of a five-coordinate high-spin complex. The heme therefore appears to be accommodated in the mutated heme pocket with an axial coordination involving His-142. Upon exposure of the rHSA(HL)–heme solution to O_2, the UV-vis absorption immediately changed to that of the O_2 adduct complex at 0–25 °C.[13,14] After introduction of CO gas, the hemoprotein produced a stable carbonyl complex.

Laser flash photolysis experiments were carried out to evaluate the kinetics of the O_2 binding to the rHSA(HL)–heme.[11,15,16] The absorbance decay accompanying the O_2 recombination to rHSA(HL)–heme was composed of single-exponential. On the other hand, the rebinding of CO followed biphasic decay, which is normally not observed in Mb. Results

of numerous investigations of synthetic model hemes have shown that a bending strain in the proximal base coordination to the central ferrous ion, the "proximal-side steric effect", can decrease the association rate for CO without greatly altering the kinetics of O_2 association.[15,16] Therefore, a possible explanation is that there are two different geometries of the axial histidine (His-142) coordination to the central ferrous ion of the heme in rHSA(HL), each one accounting for the biphasic kinetics of CO rebinding.

By analyzing the CO/O_2 competitive binding following laser flash photolysis,[15,16] we obtained the association rate constants for O_2 ($k_{on}^{O_2}$) and the O_2 binding affinities [$P_{1/2}^{O_2} = (K^{O_2})^{-1}$] for rHSA(HL)–heme (Table 1).[11] The faster phase, defined as species I, and the slower phase, defined as species II, yielded two different O_2 binding affinities. In species I, the proximal His might coordinate to the central ferrous ion without strain, whereas in species II, the ligation might involve some distortion, resulting in weaker O_2 binding (Figure 3).

Table 1. O_2 binding parameters of rHSA(mutant)–heme complexes.[a]

Hemoproteins	$10^{-6}\ k_{on}^{O_2}$ ($M^{-1}s^{-1}$)	$10^{-3}\ k_{off}^{O_2}$ (s^{-1})		$P_{1/2}^{O_2}$ (Torr)	
		I	II	I	II
rHSA(HL)–Heme	7.5	0.22	1.70	18	134
rHSA(HL/L185N)–Heme	14	0.02	0.29	1	14
rHSA(HL/R186L)–Heme	25	0.41	8.59	10	209
rHSA(HL/R186F)–Heme	21	0.29	7.01	9	203
Hb(α) (R-state)[b]	33[c]	0.013[d]		0.24	
Mb[e]	14	0.012		0.51	
RBC[f]				8	

[a] In 50 mM potassium phosphate buffered Solution (pH 7.0) at 22°C. I or II indicates species I or II.
[b] Human Hb α-subunit.
[c] In 0.1 M phosphate buffer (pH 7.0, 21.5°C); ref 17.
[d] In 10 mM phosphate buffer (pH 7.0, 20°C); ref 18.
[e] Sperm whale Mb. In 0.1 M potassium phosphate buffer (pH 7.0, 20°C); ref 19.
[f] Human red cell suspension. In isotonic buffer (pH 7.4, 20°C); ref 23.

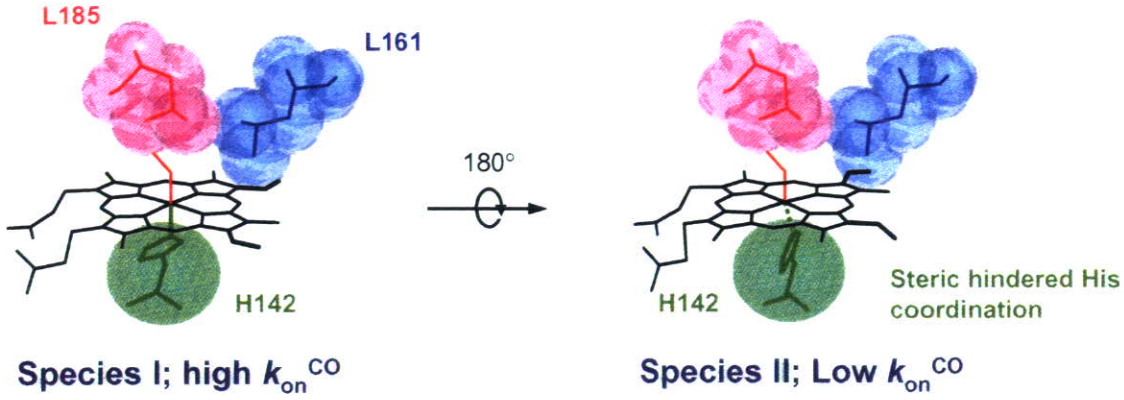

Figure 3. Structural models of heme-O_2 site of rHSA(HL)–heme complex.

The $P_{1/2}^{O_2}$ value of rHSA(HL)–heme was determined to be 18 Torr (species I), which was 35–75-fold higher (O_2 binding affinity is lower) than those of Hbα (R-state) and Mb.[17–19] This low affinity for O_2 was kinetically attributable to a 17–18-fold increases in the O_2 dissociation rate constants. The O_2 binding affinity should be adjusted to similar values for Hb and human RBC to develop this artificial hemoprotein as a blood substitute.

Introduction of Distal Base into the 185 Position

The His-64 in Hb and Mb on the distal side of the heme plays an important role for tuning their ligand affinities. A neutron diffraction study of MbO_2 showed that the N–H bond of the distal His-64 is restrained from optimal alignment for strong H–bonding with the coordinated O_2.[20] Olson and co-workers reported that the substitution of Gly for His-64 in Mb and Hb(α) caused a marked decrease in the O_2 binding affinity.[21] In view of these investigations, we reasoned that systematic variation of the steric hindrance and local polarity of the heme pocket in subdomain IB of HSA would allow modulation of the O_2 binding affinity. One approach to enhancing the O_2 binding affinity of rHSA–heme would be to introduce a basic amino acid into an appropriate position on the distal side of the heme. Our modeling results showed that the favorable position for the distal base insertion was Leu-185. Consequently, we replaced Leu-185 in rHSA(HL) [or rHSA(I142H/Y161F) [= rHSA(HF)]] with Asn, Gln, and His using site-directed mutagenesis (Figure 2b–2d).[22]

The rHSA(HL/L185N)–heme under Ar atmosphere showed a visible absorption band at 559 nm with a small shoulder at 530 nm, which was similar to the spectrum observed for rHSA(HL)–heme,[11] deoxy Mb,[13] and chelated protoheme.[14] The spectral pattern clearly indicated the formation of a five-coordinate high-spin complex. On the contrary, in the spectra of rHSA(HF/L185Q)–heme and rHSA(HF/L185H)–heme, the β band at 528 nm appeared relatively sharp, suggesting partial formation of a six-coordinate heme complex. Upon exposure of the rHSA(HL/L185N)–heme solution to O_2, the UV-vis absorption changed immediately to that of the O_2 adduct complex at 22°C. In contrast, rHSA(HF/L185Q)–heme and rHSA(HF/L185H)–heme were oxidized by O_2, even at low temperature (5°C). After introducing CO gas, all the hemoproteins produced stable carbonyl complexes with identical absorption spectral patterns.

Marked differences are apparent in the comparison of the O_2 binding parameters for rHSA(HL)–heme and rHSA(HL/L185N)–heme. The presence of Asn rather than Leu at position 185 resulted in 18-fold and 10-fold increases in the O_2 binding affinity, respectively, for species I and II (Table 1). These increases were predominantly attributable to the 6–11-fold diminution of the $k_{off}^{O_2}$ values. The high O_2 binding affinity ($P_{1/2}^{O_2}$: 1 Torr) for rHSA(HL/L185N)–heme is now close to that of Hb (R-state) (0.24 Torr) and Mb (0.5 Torr) (Table 1).

Introduction of Leu or Phe into the 186 Position

For rHSA–heme to provide effective O_2 transport *in vivo*, the affinity should be more similar to that of human RBC ($P_{1/2}^{O_2}$: 8 Torr).[23] This requires an O_2 binding affinity that is intermediate between the values of rHSA(HL)–heme and rHSA(HL/L185N)–heme. An effective means to control the O_2 binding affinity of the heme is introduction of a different polar amino acid around the O_2 binding site. A polar Arg-186 exists at the entrance of the heme pocket; we expected that insertion of a nonpolar residue at this position would change the O_2 binding affinity of rHSA–heme. Consequently, we designed new triple mutants, rHSA(HL/R186L) and rHSA(HL/R186F) (Figure 2e,2f).

The MCD in the Soret band region of the ferric rHSA(HL/R186L)–hemin and rHSA(HL/R186F)–hemin both showed low intensity, which is fundamentally equivalent to that observed for rHSA(HL)–hemin. The reduced ferrous form demonstrated the characteristic

UV-vis absorption and MCD spectra of the five-coordinate high-spin complex under an Ar atmosphere. Upon bubbling O_2 gas through the solutions, the spectral patterns were shifted to that of the O_2 adduct complex. The distinct features of all the spectra were quite similar to those of the rHSA(HL)–heme. Fortunately, the O_2 binding affinities of rHSA(HL/R186L)–heme and rHSA(HL/R186F)–heme were more similar to that of human RBC ($P_{1/2}^{O_2}$: 8 Torr) (Table 1). We can conclude that the Arg-186 is an important key amino acid to control the O_2 binding property of the heme and the obtained triple mutants could become RBC substitutes.

Conclusion

We have shown clearly that rHSA–heme can be engineered to bind O_2 reversibly. However, the complex did not display optimal O_2 binding affinity. By emphasizing modification on the distal side of the heme pocket in rHSA, we have prepared distinct rHSA(triple mutant)–heme complexes with a broad range of O_2 binding affinities. The highest affinity mutant rHSA(HL/L185N) contains Asn-185, which has a short amide side-chain that enhances the O_2 binding affinity. On the other hand, introduction of the larger Gln and His side-chains at position 185 partly provided a six-coordinate heme character, and did not stabilize O_2 binding. In a different approach, substitution of Arg-186 at the entrance of the heme pocket with Leu or Phe provided a useful reduction in the O_2 binding affinity, yielding $P_{1/2}^{O_2}$ values that are closely resemble that of the human RBC.

The transport of O_2 by rHSA–heme could be of great clinical importance, not only as a blood substitute, but also as an O_2-providing therapeutic reagent. If the HSA-based O_2 carrier is realized, it has the potential of acting not only as a RBC substitute, but also as an O_2 providing therapeutic reagent.

This work was supported by PRESTO "Control of Structure and Functions", JST, and Health Science Research Grants (Regulatory Science) from MHLW Japan. The work at Imperial College London was partially carried out through the Japan-UK Research Cooperative Program (Joint Project) of JSPS. The authors acknowledge to Dr. Stephen Curry and Dr. Patricia A. Zunszain for their valuable suggestions related to molecular designs of the rHSA mutants and site-directed mutagenesis.

References

[1] Peters Jr., T. *"All about Albumin, Biochemistry, Genetics and Medical Applications"*, Academic Press, San Diego 1997.

[2] (a) U. Kragh-Hansen, *Pharmacol. Rev.* **1981**, *33*, 17. (b) U. Kragh-Hansen, *Danish Med. Bull.* **1990**, *37*, 57.

[3] (a) S. Curry, H. Madelkow, P. Brick, N. Franks, N. *Nat. Struct. Biol.* **1998**, *5*, 827. (b) A. A. Bhattacharya, T. Grune, S. Curry, *J. Mol. Biol.* **2000**, *303*, 721.

[4] J. Ghuman, P. A. Zunszain, I. Petipas, A. A. Bhattacharya, M. Otagiri, S. Curry, *J. Mol. Biol.* **2005**, *353*, 38.

[5] P. A. Adams, M. C. Berman, *Biochem. J.* **1980**, *191*, 95.

[6] M. C. Marden, E. S. Hazard, L. Leclerc, Q. H. Gibson, *Biochemistry* **1989**, *28*, 4422.

[7] T. Komatsu, Y. Matsukawa, E. Tsuchida, *Bioconjugate Chem.* **2002**, *13*, 397.

[8] He, X. M.; Carter, D. C. *Nature* **1992**, *358*, 209–215.

[9] P. A. Zunszain, J. Ghuman, T. Komatsu, E. Tsuchida, S. Curry, *BMC Struct. Biol.* **2003**, *3*: 6.

[10] M. Wardell, Z. Wang, J. X. Ho, J. Robert, F. Ruker, J. Rubel, D. C. Carter, *Biochem. Biophys. Res. Commun.* **2002**, *291*, 813.

[11] (a) T. Komatsu, N. Ohmichi, P. A. Zunszain, S. Curry, E. Tsuchida, *J. Am. Chem. Soc.* **2004**, *126*, 14304. (b) T. Komatsu, N. Ohmichi, A. Nakagawa, P. A. Zunszain, S. Curry, E. Tsuchida, *J. Am. Chem. Soc.* **2005**, *127*,15933.

[12] L. Vickery, T. Nozawa, K. Sauer, *J. Am. Chem. Soc.* **1976**, *98*, 343.

[13] E. Antonini, M. Brunori, M. "*Hemoglobin and Myoglobin in Their Reactions with Ligands*"; North-Holland Pub., Amsterdam 1971; pp 18.

[14] T. G. Traylor, C. K. Chang, J. Geibel, A. Berzinis, T. Mincey, J. Cannon, *J. Am. Chem. Soc.* **1979**, *101*, 6716.

[15] J. P. Collman, J. I. Brauman, B. L. Iverson, J. L. Sessler, R. M. Moris, Q. H. Gibson, *J. Am. Chem. Soc.* **1983**, *105*, 3052.

[16] T. G. Traylor, S. Tsuchiya, D. Campbell, M. Mitchel, D. Stynes, N. Koga, *J. Am. Chem. Soc.* **1985**, *107*, 604.

[17] Q. H. Gibson, *J. Biol. Chem.* **1970**, *245*, 3285.

[18] J. H. Olson, M. E. Andersen, Q. H. Gibson, *J. Biol. Chem.* **1971**, *246*, 5919.

[19] R. Rohlfs, A. J. Mathews, T. E. Carver, J. S. Olson, B. A. Springer, K. D. Egeberg, S. G. Sliger, *J. Biol. Chem.* **1990**, 265, 3168.

[20] S. E. V. Phillips, B. P. Schoenborn, *Nature* **1981**, *292*, 81.

[21] J. S. Olson, A. J. Mathews, R. J. Rohlfs, B. A. Springer, K. D. Egeberg, S. G. Sligar, J. Tame, J.-P. Renaud, K. Nagai, *Nature* **1988**, *336*, 365.

[22] T. Komatsu, A. Nakagawa, P. A. Zunszain, S. Curry, E. Tsuchida, *J. Am. Chem. Soc.* **2007**, *129*, in press.

[23] K. Imai, H. Morimoto, M. Kotani, H. Watari, W. Hirata, M. Kuroda, *Biochim. Biphys. Acta.* **1970**, *200*, 189.

ohio1/ybc-ybc/ybc-ybc/ybc99907/ybc2461d07z | xppws | 23:ver.3 | 1/7/08 | 20:23 | Msc: bc-2007-00400n | TEID: ajk00 | BATID: bc1a60

O_2 Binding to Human Serum Albumin Incorporating Iron Porphyrin with a Covalently Linked Methyl-L-Histidine Isomer

Akito Nakagawa,[†] Teruyuki Komatsu,*[,†,‡] Makoto Iizuka,[†] and Eishun Tsuchida*[,†]

Research Institute for Science and Engineering, Waseda University, 3-4-1 Okubo, Shinjuku-ku, Tokyo 169-8555, Japan, and PRESTO, Japan Science and Technology Agency (JST), 4-1-8 Honcho, Kawaguchi-shi, Saitama 332-0012, Japan. Received October 30, 2007; Revised Manuscript Received December 1, 2007

We describe the significant difference in the O_2 binding affinities of human serum albumin (HSA) incorporating 5,10,15,20-tetrakis{α,α,α,α-*o*-(1′-methylcyclohexanamido)phenyl}porphinatoiron(II) with a covalently linked 1-methyl-L-histidine or 3-methyl-L-histidine [HSA-FeP(1-MHis), HSA-FeP(3-MHis)]. The HSA-FeP(3-MHis) showed an extraordinarily high O_2 binding affinity ($P_{1/2}$ = 0.2 Torr, 25 °C, pH 7.4), which is close to those of relaxed-state hemoglobin and myoglobin. However, replacement of the 3-methyl-L-histidine moiety in FeP(3-MHis) by 1-methyl-L-histidine caused a 35-fold reduction in O_2 affinity; the $P_{1/2}$ value of HSA-FeP(1-MHis) (22 Torr, 37 °C, pH 7.4) is almost identical to that of human red blood cells. Results of kinetic studies indicate that the low O_2 binding affinity of FeP(1-MHis) is predominantly manifested in the high O_2 dissociation rate constant. In a toluene solution, an identical relationship in the O_2 binding property was similarly observed for FeP(1-MHis) and FeP(3-MHis). The axial Fe-N(1-MHis) coordination might be restrained by steric interaction between the 4-methylene group of the histidine and the porphyrin plane.

INTRODUCTION

Numerous synthetic model hemes have been prepared to mimic the O_2 binding capability of hemoglobin (Hb) and myoglobin (Mb) over the past few decades (*1–3*). In these highly modified iron(II) porphyrins, axial coordination of the nitrogenous base plays a crucial role in regulating O_2 binding affinity. Collman and co-workers demonstrated that picket-fence porphyrin[1] ligating a 1,2-dimethylimidazole (1,2-DMIm) showed a 70-fold lower O_2 binding affinity [$P_{1/2}$ (O_2 partial pressure at which 50% of porphyrin was dioxygenated) = 38 Torr, 25 °C] than that of the complex with 1-methylimidazole (1-MIm) (*4, 5*). This reduction was ascribed to the steric interaction between the 2-methyl group of the imidazole and the porphyrin plane. Furthermore, they showed that the replacement of imidazole by pyridine in the tailed picket-fence porphyrin lowered the O_2-binding affinity by a factor of 40 (*6*). The weaker π-basicity of pyridine and the increased steric repulsion of the six-atom pyridine ring compared to that of the five-atom imidazole reduced the O_2 binding of the iron(II) porphyrins (*7–10*). We previously reported that 2-[{8-*N*-(methylimidazolyl)octanoyloxy}methyl]-5,10,15,20-tetrakis{α,α,α,α-*o*-(1′-methylcyclohexanamido)phenyl}porphinatoiron(II) [FeP(2-MIm)] formed a stable O_2 adduct in toluene solution, and human serum albumin (HSA) incorporating FeP(2-MIm) [HSA-FeP(2-MIm)] can bind O_2 not only in aqueous media (pH 7.4) but also in the blood stream as an artificial red blood cell (RBC) substitute (*11, 12*). For practical biomedical applications of the synthetic iron(II) porphyrin as an O_2 carrier, two physiological requirements exist. First, O_2 binding affinity should be close to that of human RBC ($P_{1/2}$ = 27 Torr, 37 °C). Second, it is favorable to use natural histidine as an axial base because some imidazole and pyridine derivatives show toxicity to respiratory organs and the central nervous system (*13*). Nevertheless, few studies have addressed O_2 binding of the synthetic model heme having a histidyl group (*14–16*). We have demonstrated the O_2 binding equilibrium and kinetics of 5,10,15,20-tetrakis{α,α,α,α-*o*-(1′-methylcyclohexanamido)phenyl}porphinatoiron(II) with an ω-histidylalkyl chain [FeP(His)[2]] (*17*). A new class of biocompatible O_2 carriers would be realized if we can regulate O_2 binding affinity by changing the steric and electronic natures of the attached histidine. We now report a significant difference in the O_2 binding properties of HSA hybrid with synthetic iron(II) porphyrin bearing a covalently linked 1-methyl-L-histidine or 3-methyl-L-histidine [HSA-FeP(1-MHis) and HSA-FeP(3-MHis)] (Figure 1) under physiological conditions (pH 7.4, 37 °C).

The 1-methyl-L-histidine methylester or 3-methyl-L-histidine methylester was introduced into the carboxyl group of the parent free-base porphyrin, 2-{(4-carboxybutanoyloxy)methyl}-5,10,15,20-tetrakis{α,α,α,α-*o*-(1′-methylcyclohexanamido)phenyl}porphin [2HP(COOH)] (*11*), via an amide linkage, yielding histidine-terminated porphyrins (>60% yield) (Figure 1). The cyclohexanoyl substituents stabilized the O_2 adduct complex rather than the pivaloy group (*11*). The central iron was inserted as iron(II) using $FeBr_2$ and 2,6-lutidine in anhydrous THF. The analytical data of all compounds were satisfactorily obtained (see Supporting Information).

Both FeP(1-MHis) and FeP(3-MHis) are readily incorporated into HSA (Mw: 66.5 kDa), producing stable artificial hemoproteins: HSA-FeP(1-MHis) and HSA-FeP(3-MHis) [in phos-

* Corresponding author. Tel: +81-3-5286-3120. Fax: +81-3-3205-4740. E-mail: eishun@waseda.jp (E.T.). E-mail: teruyuki@waseda.jp (T.K.).

† Waseda University.

‡ Japan Science and Technology Agency (JST).

[1] Picket-fence porphyrin: 5,10,15,20-tetrakis{(α,α,α,α-o-pivalamido)phenyl}porphinatoiron.

[2] Abbreviations: FeP(His), 2-{(4-methoxycarbonyl-histidinamidobutanoyloxy)methyl}-5,10,15,20-tetrakis{α,α,α,α-o-(1′-methyl)cyclohexanamido)phenyl}porphinatoiron; FeP(1-MHis),2-[{4-methoxycarbonyl(1-methyl)histidinamidobutanoyloxy}methyl]-5,10,15,20-tetrakis{α,α,α,α-o-(1′-methyl)cyclohexanamido)phenyl}porphinatoiron; FeP(3-MHis),2-[{4-methoxycarbonyl(3-methyl)histidinamidobutanoyloxy}methyl]-5,-10,15,20-tetrakis{α,α,α,α-o-(1′-methylcyclohexanamido)phenyl}porphinatoiron.

10.1021/bc700400n CCC: $37.00

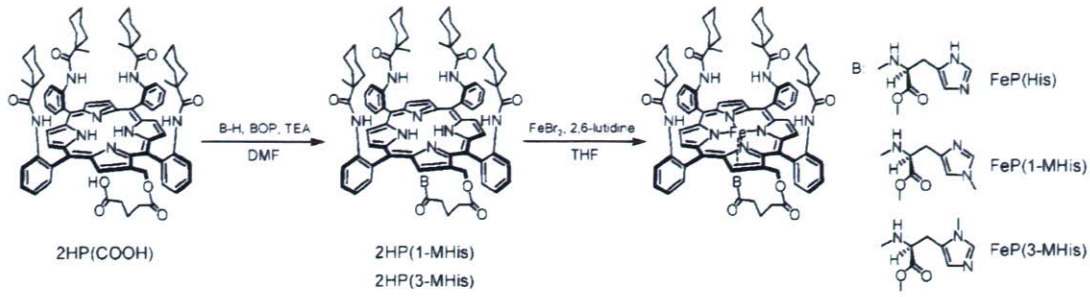

Figure 1. Synthetic scheme of iron(II) porphyrin bearing a covalently linked histidine derivative as an axial base at the β-pyrrolic position.

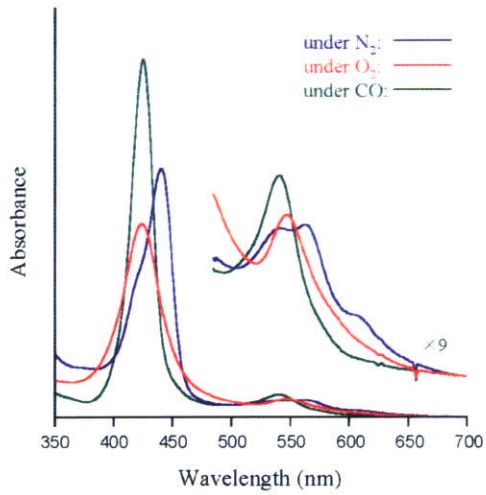

Figure 2. UV–vis absorption spectral changes of HSA-FeP(1-MHis) in PBS solution at 25 °C.

phate-buffered saline (PBS) solution at pH 7.4, [porphyrin]/[HSA] = 4 (mol/mol)]. The UV–vis absorption spectra of the aqueous HSA-FeP(1-MHis) and HSA-FeP(3-MHis) solutions under an N_2 atmosphere showed a similar feature of HSA-FeP(2-MIm) and HSA-FeP(His) (Figure 2) (Table S1) (*11, 17*). The spectral shapes resembled those of the five-N-coordinate high-spin ferrous complex of picket-fence porphyrin and other tetraphenylporphyrin derivatives (*5*). These results indicated that FeP(1-MHis) and FeP(3-MHis) formed a five-N-coordinate high-spin complex with an intramolecularly coordinated methyl-L-histidine moiety in the protein matrix. Upon bubbling of O_2 gas into the solution, the absorption pattern changed immediately to that of the O_2 adduct complex. The dioxygenations of these artificial hemoproteins have been observed reversibly under physiological conditions (pH 7.4, 37 °C). After passing the CO gas, the absorption maxima shifted to that of the carbonyl complex.

The O_2 binding affinities [$K = (P_{1/2})^{-1}$] of HSA-FeP(1-MHis) and HSA-FeP(3-MHis) were determined by the absorption spectral changes at various O_2 concentrations (eq 1).

$$\mathrm{FeP(B)} + \mathrm{O_2} \underset{k_{off}}{\overset{k_{on}}{\rightleftharpoons}} \mathrm{FeP(B)\text{-}O_2} \qquad [K = (P_{1/2})^{-1}] \tag{1}$$

The HSA-FeP(3-MHis) showed an extraordinarily high O_2 binding affinity ($P_{1/2}$ = 0.2 Torr, 25 °C), which is 5-fold greater than that of HSA-FeP(His), which was close to the values of the relaxed-state Hb(α) and Mb (Table 1) (*18–20*). However, replacement of the 3-methyl-L-histidine moiety in FeP(3-MHis) by the 1-methyl-L-histidine isomer [FeP(1-MHis)] caused a 35-fold reduction of O_2 binding affinity ($P_{1/2}$ = 7 Torr, 25 °C); the

Table 1. O_2 Binding Parameters of Human Serum Albumin Hybrid with Iron(II) Porphyrin Bearing a Methyl-L-Histidine Isomer in PBS Solution (pH 7.4) at 25 °C

HSA-iron(II) porphyrin	k_{on} (M^{-1} s^{-1})	k'_{on} (M^{-1} s^{-1})	k_{off} (s^{-1})	k'_{off} (s^{-1})	$P_{1/2}$[a] (Torr)
HSA-FeP(1-MHis)	5.4×10^7	8.1×10^6	620	93	7 (22)
HSA-FeP(3-MHis)	5.4×10^7	6.8×10^6	20	2.4	0.2 (1)
HSA-FeP(His)[b]	5.4×10^7	8.8×10^6	89	14	1 (3)
Hb(α) (R-state)[c]	3.3×10^7[d]		13[e]		0.24
Mb[f,g]	1.4×10^7		12		0.51
RBC[h]					8 (27)

[a] At 37 °C in parenthesis. [b] Ref *11*. [c] Human Hb α-subunit. [d] In 0.1 M phosphate buffer (pH 7.0, 21.5 °C); ref *18*. [e] In 10 mM phosphate buffer (pH 7.0, 20 °C); ref *19*. [f] Sperm whale Mb. [g] In 0.1 M phosphate buffer (pH 7.0, 20 °C); ref *20*. [h] Human red blood cell suspension. In isotonic buffer (pH 7.4); ref *21*.

$P_{1/2}$ value of 22 Torr at 37 °C was almost identical to that of human RBC (27 Torr) (*21*).

Laser flash photolysis experiments gave the association and dissociation rate constants for O_2 (k_{on}, k_{off}) (*5, 11*). The time course of the absorption change accompanying the O_2 recombinations to HSA-FeP(1-MHis) and HSA-FeP(3-MHis) after the laser pulse irradiation comprised two phases of first-order kinetics (Figure S1a). The decay was fitted by a double exponential profile, which provided the fast and slow association rate constants of O_2 (k_{on} and k'_{on}) (Table 1). This behavior was similarly observed in HSA-FeP(His) and HSA-FeP(2-MIm) (*11*). It has been interpreted that the O_2 associations to the iron(II) porphyrins in HSA were affected by microenvironments around the accommodation site (steric hindrance of the amino acid residue and difference in polarity) (*22*). The kinetic data indicated that the low O_2 binding affinity of HSA-FeP(1-MHis) is predominantly manifested in the high O_2 dissociation rate constant (Table 1).

To evaluate the significant differences in FeP(1-MHis) and FeP(3-MHis), their O_2 binding parameters in toluene solution were determined. The UV–vis absorption spectra of ferrous FeP(1-MHis) (λ_{max}, 440, 542, 563 nm) and FeP(3-MHis) (λ_{max}, 440, 540, 565 nm) under an N_2 atmosphere showed the formation of a five-N-coordinate high spin complex. Dioxygenation was sufficiently stable and reversible at 25 °C depending on O_2 partial pressure. The recombination process of O_2 to the iron(II) porphyrins in toluene solution after laser flash photolysis was fitted by a single exponential (Figure S1b). FeP(3-MHis) exhibited a 6-fold higher O_2 binding affinity ($P_{1/2}$ = 0.3 Torr, 25 °C) compared to that of FeP(His) (Table 2) (*11*). Kinetically, this high O_2 binding affinity is attributable to the low O_2 dissociation rate. The high σ-basicity of 3-methyl-L-histidine (p*K*a, 6.48) in comparison to that of histidine (p*K*a, 6.00) (*23*) can serve to increase the electron density on the central metal, which would enhance O_2 uptake. FeP(1-MHis) showed a 90-fold lower O_2 affinity ($P_{1/2}$ = 27 Torr, 25 °C) relative to FeP(3-MHis), which is mainly caused by the high k_{off} value, as observed in aqueous media. In general, the steric

Table 2. O_2 Binding Parameters of Iron(II) Porphyrin Bearing a Methyl-L-Histidine in Toluene Solution at 25 °C

iron(II) porphyrin	k_{on} (M^{-1} s^{-1})	k_{off} (s^{-1})	$P_{1/2}$ (Torr)
FeP(1-MHis)	9.8×10^7	3.5×10^4	27
FeP(3-MHis)	1.6×10^8	5.2×10^2	0.3
FeP(His)[a]	2.0×10^8	4.3×10^3	1.7

[a] In benzene solution, ref *17*.

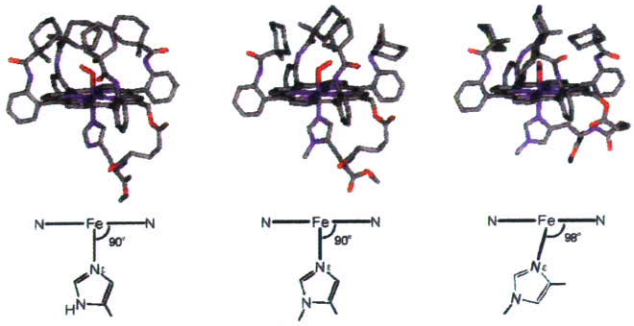

Figure 3. Simulated structures of the O_2 adduct complexes of FeP(His), FeP(3-MHis), and FeP(1-MHis). In FeP(His) and FeP(3-MHis), the bond angles of N(por)−Fe−N(His) were 90°, but 98° in FeP(1-MHis) because of the steric interaction between the 4-methylene group of histidine and the porphyrin plane. Molecular dynamics and minimization (force field: esff) were performed using an Insight II system. Hydrogens were omitted for clarification.

hindrance to the axial base coordination deforms the six-coordinate structure of the iron(II) porphyrin and increases the O_2 dissociation rate constant (*1, 2*). For example, the 1,2-DMIm complexes showed 11–58-fold higher k_{off} values than the 1-MIm ligated complexes (*3, 5, 24*).

We simulated the geometry of histidine coordination in dioxygenated porphyrin.[3] The bond angle of N(por)−Fe−N(His) was 90° for FeP(His) and FeP(3-MHis), but it was markedly tilted in FeP(1-MHis) (a maximum of 98°) (Figure 3). On the basis of these results, it can be concluded that the axial coordination of 1-methyl-L-histidine to the central iron is restrained by the steric interaction between the 4-methylene group of the histidine and the porphyrin plane, which significantly increased the dissociation rate of O_2.

In conclusion, a variation in the methyl-L-histidine isomer covalently linked at the porphyrin periphery changed the O_2 binding affinity of the iron(II) porphyrin by a factor of 90 in toluene. This difference is greater than the previous finding for a picket-fence porphyrin (2-MIm) complex-bound O_2 with a 70-fold lower affinity than that of the 1-MIm complex (*4*). The increased k_{off} value of FeP(1-MHis) is caused by steric repulsion between the 4-methylene group of histidine and the porphyrin plane. In aqueous media, the O_2 binding ability of HSA incorporating the iron(II) porphyrin can also be modulated by structural isomerization of the axial methyl-L-histidine. HSA-FeP(1-MHis) with a $P_{1/2}$ value similar to that of human RBC under physiological conditions can become a promising O_2 carrier, which satisfies both the biocompatibility and clinical requirements for efficient O_2 delivery to the tissue cells.

ACKNOWLEDGMENT

This work was partially supported by Grant-in-Aid for Young Scientists (B) (No. 18750156) from JSPS, PRESTO from JST, and Health Science Research Grants from MHLW, Japan.

[3] The esff forcefield simulation was performed using an Insight II system (Molecular Simulations Inc.). The structure was generated by alternative minimizations and annealing dynamic calculations from 1,000 to 100 K.

Supporting Information Available: Experimental details, absorption maximum wavelengths of the iron(II) porphyrins, and absorption change accompanying O_2 rebinding to FeP(3-MHis) and HSA-FeP(3-MHis) after laser flash photolysis. This material is available free of charge via the Internet at http://pubs.acs.org.

LITERATURE CITED

(1) Collman, J. P., Boulatov, R., Sunderland, C. J., and Fu, L. (2004) Functional analogues of cytochrome c oxidase, myoglobin, and hemoglobin. *Chem. Rev. 104*, 561–588.

(2) Collman, J. P., and Fu, L. (1999) Synthetic Models for Hemoglobin and Myoglobin. *Acc. Chem. Res. 32*, 455–463.

(3) Momenteau, M., and Reed, C. A. (1994) Synthetic heme-dioxygen complexes. *Chem. Rev. 94*, 659–698.

(4) Collman, J. P., Brauman, J. I., Doxsee, K. M., Halberd, T. M., and Suslick, K. S. (1978) Model compounds for the T state of hemoglobin. *Proc. Natl. Acad. Sci. U.S.A. 75*, 564–568.

(5) Collman, J. P., Brauman, J. I., Iverson, B. L., Sessler, J. L., Morris, R. M., and Gibson, Q. H. (1983) O_2 and CO binding to iron(II) porphyrins: A comparison of the "picket fence" and "pocket" porphyrins. *J. Am. Chem. Soc. 105*, 3052–3064.

(6) Collman, J. P., Brauman, J. I., Doxsee, K. M., Sessler, J., Morris, R. M., and Gibson, Q. H. (1983) Effect of axial base on dioxygen and carbon monoxide affinities of iron(II) porphyrins. Imidazole vs. pyridine. *Inorg. Chem. 22*, 1427–1432.

(7) Chang, C. K., and Traylor, T. G. (1975) Kinetics of oxygen and carbon monoxide binding to synthetic analogs of the myoglobin and hemoglobin active sites. *Proc. Nat. Acad. Sci. U.S.A. 72*, 1166–1170.

(8) Linard, J. E., Ellis, P. E., Jr., Budge, J. R., Jones, R. D., and Basolo, F. (1980) Oxygenation of iron(II) and cobalt(II) "capped" porphyrins. *J. Am. Chem. Soc. 102*, 1896–1904.

(9) Momenteau, M., Mispelter, J., Loock, B., and Lhoste, J.-M. (1985) Both-faces hindered porphyrins. Part 3. Synthesis and characterization of internally five-co-ordinated iron(II) basket handle porphyrins derived from 5,10,15,20-tetrakis(o-aminophenyl)porphyrin. *J. Chem. Soc., Perkin Trans.1* 221–231.

(10) Lavalette, D., Tetreau, C., Mispelter, J., Momenteau, M., and Lhoste, J.-M. (1984) Linear free-energy relationships in binding of oxygen and carbon monoxide with heme model compounds and heme proteins. *Eur. J. Biochem. 145*, 555–565.

(11) Komatsu, T., Matsukawa, Y., and Tsuchida, E. (2002) Effect of heme structure on O_2-binding properties of human serum albumin-heme hybrids: Intramolecular histidine coordination provides a stable O_2-adduct complex. *Bioconjugate Chem. 13*, 397–402.

(12) Komatsu, T., Huang, Y., Yamamoto, H., Horinouchi, H., Kobayashi, K., and Tsuchida, E. (2004) Exchange transfusion with synthetic oxygen-carrying plasma protein "albumin-heme" into an acute anemia rat model after seventy-percent hemodilution. *J. Biomed. Mater. Res. 71A*, 644–651.

(13) Sax, N. I., and Lewis, R. J. (1987) *Hazardous Chemicals Desk Reference*, Van Nostrand Reinhold Company, Inc., New York.

(14) Van der Heijden, A., Peter, H. G., and Van der Oord, A. H. A. (1971) Coupling of L-histidine methyl ester and L-histidine-containing peptide esters to ferric protoporphyrin IX chloride. *J. Chem. Soc. D* 369–370.

(15) Warme, P. K., and Hager, L. P. (1970) Heme sulfuric anhydrides. I. Synthesis and reactions of mesoheme sulfuric anhydride. *Biochemistry 9*, 1599–1606.

(16) Momenteau, M., Rougee, M., and Loock, B. (1976) Five-coordinate iron-porphyrin as a model for the active site of hemoproteins. Characterization and coordinating properties. *Eur. J. Biochem. 71*, 63–76.

(17) Komatsu, T., Matsukawa, Y., Miyatake, K., and Tsuchida, E. (2001) O_2-adduct complex of meso-tetrakis(α,α,α,α-o-pivalamidophenyl)porphinatoiron(II) with an intramolecularly coordinated proximal histidine. *Chem. Lett.* 668–669.

(18) Gibson, Q. H. (1970) The reaction of oxygen with hemoglobin and the kinetic basis of the effect of salt on binding of oxygen. *J. Biol. Chem. 245*, 3285–3288.

(19) Olson, J. S., Andersen, M. E., and Gibson, Q. H. (1971) The Dissociation of the first oxygen molecule from some mammalian oxyhemoglobins. *J. Biol. Chem. 246*, 5919–5923.

(20) Rohlfs, R., Mathews, A. J., Carver, T. E., Olson, J. S., Springer, B. A., Egeberg, K. D., and Sligar, S. G. (1990) The effects of amino acid substitution at position E7 (residue 64) on the kinetics of ligand binding to sperm whale myoglobin. *J. Biol. Chem. 265*, 3168–3176.

(21) Imai, K., Morimoto, H., Kotani, M., Watari, H., Hirata, W., and Kuroda, M. (1979) Studies on the function of abnormal hemoglobins I. An improved method for automatic measurement of the oxygen equilibrium curve of hemoglobin. *Biochim. Biophys. Acta 200*, 189–1967.

(22) Komatsu, T., Matsukawa, Y., and Tsuchida, E. (2000) Kinetics of CO and O_2 binding to human serum albumin-heme hybrid. *Bioconjugate Chem. 11*, 772–776.

(23) Lide, R. D., Eds. (2000) *CRC Handbook of Chemistry and Physics*, 81st ed., Section 7, CRC Press, Boca Raton, FL.

(24) Momenteau, M., Loock, B., Tetreau, C., Lavalette, D., Croisy, A., Schaeffer, C., Huel, and Lhoste, J.-M. (1987) Synthesis and characterization of a new series of iron(II) single-face hindered porphyrins. Influence of central steric hindrance upon carbon monoxide and oxygen binding. *J. Chem. Soc., Perkin Trans. 2* 249–257.

BC700400N

Journal of Surgical Research xx, xxx (2008)
doi:10.1016/j.jss.2007.12.770

Systemic Administration of Hemoglobin Vesicle Elevates Tumor Tissue Oxygen Tension and Modifies Tumor Response to Irradiation

M. Yamamoto, M.D.,* Y. Izumi, M.D., Ph.D.,*,[1] H. Horinouchi, M.D., Ph.D.,* Y. Teramura, Ph.D.,§ H. Sakai, Ph.D.,§ M. Kohno, M.D., Ph.D.,* M. Watanabe, M.D., Ph.D.,* M. Kawamura, M.D., Ph.D.,* T. Adachi, M.D., Ph.D.,† E. Ikeda, M.D., Ph.D.,‡ S. Takeoka, Ph.D.,§ E. Tsuchida, Ph.D.,§ and K. Kobayashi, M.D., Ph.D.*

*Division of General Thoracic Surgery, Department of Surgery; †Department of Biochemistry and Integrative Medical Biology; ‡Department of Pathology, School of Medicine, Keio University, Tokyo, Japan; and §Research Institute for Science and Engineering, Waseda University, Tokyo, Japan

Submitted for publication September 22, 2007

Background. **We have developed a phospholipid liposome vesicle encapsulating concentrated human hemoglobin (hemoglobin vesicle, HbV) as an artificial oxygen carrier, as an alternative to red cell transfusion. We have verified its oxygen transporting capability in a variety of preclinical models. Recent evidence suggests that artificial oxygen carriers may also be applicable for better oxygenation of ischemic or hypoxic tissues including tumors. To our knowledge, tumor oxygenation using a liposome-type artificial oxygen carrier has not been closely tested. In the present study, we tested whether systemic HbV administration changes tumor tissue oxygen tension, and if it modifies tumor response to irradiation.**

Materials and methods. **Lewis lung carcinoma was grown subcutaneously in the left hindleg of C57/BL6 mice. Experiments were initiated when the tumors reached approximately 8 mm. All experiments were done under room air. Tumor tissue oxygen tension was measured by phosphorescence quenching up to 45 min after systemic sample administration (saline: $n = 5$; HbV: $n = 5$; HbV containing methemoglobin (metHbV): $n = 4$; HbV with low oxygen affinity (lowP50HbV): $n = 8$) and compared between samples. To test the effects on irradiation response, samples (saline: $n = 7$; HbV: $n = 7$; metHbV: $n = 7$; lowP50HbV: $n = 7$) were administered prior to single 20-Gy irradiation, and tumor growth was compared.**

Results. **Tumor tissue oxygen tension transiently increased approximately 2-fold after HbV administration in comparison to other samples. Tumor growth was marginally delayed after irradiation by prior administration of HbV in comparison to other samples. HbV administration without irradiation did not affect significant tumor growth delay.**

Conclusions. **These results correlatively suggest that HbV augmented tumor growth delay following irradiation, at least in part, by affecting tumor tissue oxygen tension.**

Key Words: **hemoglobin vesicle; artificial oxygen carrier; tumor oxygenation; radiosensitizer; liposome; HIF1alpha.**

INTRODUCTION

Artificial oxygen carriers are currently being actively developed for use as transfusion alternatives. Artificial oxygen carriers do not have blood types, are free of potential infectious pathogens, and can be stored much longer than red blood cells (RBCs) [1]. Several preclinical studies indicate that they can be effectively applied as temporal resuscitative fluids, and some are undergoing clinical trials [2, 3].

Hemoglobin (Hb)-based oxygen carriers are classified into acellular chemically modified Hbs and encapsulated Hbs [4, 5]. We have developed a phospholipid liposome vesicle encapsulating concentrated human hemoglobin (hemoglobin vesicle, HbV) as an artificial oxygen carrier [1]. The cellular structure of HbV has characteristics that resemble those of RBCs. It has lipid bilayer membranes that prevent the direct contact of hemoglobin with blood components and the en-

[1] To whom correspondence and reprint requests should be addressed at Division of General Thoracic Surgery, Department of Surgery, School of Medicine Keio University, 35 Shinanomachi, Shinjuku-ku, Tokyo 160-8582, Japan. E-mail: yotaro@sc.itc.keio.ac.jp.

0022-4804/08 $34.00

dothelial lining, thus shielding the side effects of molecular hemoglobin [6, 7]. HbV particles are eventually captured by the phagocytes in the reticuloendothelial system and are metabolized through existing physiological pathways [8–10]. We have studied the oxygen transporting capabilities of HbV using several exchange transfusions, and hemorrhagic shock animal models [11–15]. In these studies, we have shown that HbV effectively restores the systemic circulation similar to red cell transfusion. Recently, evidence is accumulating that artificial oxygen carriers may be potentially applicable as so-called oxygen therapeutics, which enable oxygenation of ischemic tissues [16, 17]. Increasing tumor tissue oxygen tension is one such possibility. In the present study, we show that systemic administration of HbV transiently increases tumor tissue oxygen tension and modifies tumor response to irradiation.

MATERIALS AND METHODS

Preparation of Hemoglobin Vesicles

Preparation of poly(ethylene glycol) modified HbV was performed at Waseda University under sterile conditions as previously reported [18–20]. Hemoglobin was purified from outdated donated blood provided by Japanese Red Cross Society (Tokyo, Japan). The encapsulated hemoglobin (38 g/dL) contained 14.7 mmol/L of pyridoxal 5′-phosphate (PLP; Sigma, St. Louis, MO) as an allosteric effector at a molar ratio of Hb/PLP = 2.5. The lipid bilayer was composed of a mixture of 1,2-dipalmitoyl-*sn*-glycero-3-phosphatidylcholine, cholesterol, and 1,5-bis-*O*-hexadecyl-*N*-succinyl-L-glutamate at a molar ratio of 5/5/1 (Nippon Fine Chemicals, Osaka, Japan) and 1,2-distearoyl-*sn*-glycero-3-phosphatidylethanolamine-*N*-poly(ethylene glycol) (NOF Corp., Tokyo, Japan; 0.3 mol% of the total lipid). HbV was suspended in saline at the Hb concentration of 10 g/dL. The physicochemical parameters of the HbV were as follows: particle diameter, 251 ± 80 nm; methemoglobin concentration, <1%; HbCO concentration, <2%; and oxygen affinity (P_{50}), 29 Torr.

Preparation of Methemoglobin Vesicles

Methemoglobin vesicles (metHbV) were formed by oxidation of hemoglobin contained within HbV (methemoglobin formation), using the oxidative properties of nitrosylhemoglobin [21]. Nitric oxide gas was infused into the deoxygenated HbV suspension to transform hemoglobin to nitrosylhemoglobin. After infusion of nitrogen gas to expel the excess nitric oxide, oxygen was infused to convert nitrosylhemoglobin to methemoglobin, yielding metHbV. Vesicle properties were considered to be equivalent to HbV except for its lack of oxygen transporting ability.

Preparation of Low P50 Hemoglobin Vesicles

HbV with P_{50} of approximately 8 Torr (lowP50HbV) was prepared in the same way as HbV except that pyridoxal 5′-phosphate was not added. Particle diameter was controlled to 250 ± 64 nm. Vesicle properties were considered to be equivalent to HbV except for its P_{50}.

Animal and Tumor

Male C57/BL6 mice, approximately 9 weeks old, weighing 21 to 25 g (Oriental Yeast Co., Tokyo, Japan) were used for the experiment. The animals were housed five per cage in a specific pathogen-free, temperature-controlled, 12-h light/dark-cycled room with free access to food and water. For the experiments, the animals were anesthetized with intramuscular injection of a cocktail of 90 mg ketamine hydrochloride (Parke-Davis, Morris Plains, NJ) and 9 mg xylazine (Fermentia, Kansas City, MO) per kilogram body weight.

Lewis lung carcinoma cell line (Dainippon Sumitomo Pharma Co., Tokyo, Japan) was used for this study. In a separate group of donor mice, the tumors were grown subcutaneously and passaged. Under anesthesia, an approximately 1-mm-diameter tumor fragment was taken from the donor mouse and was placed subcutaneously in the left hindleg of mice in the experiment groups. Experiments were initiated 10 days after tumor implantation, at which time the tumors reached approximately 8 mm in diameter.

For material administration, the tail vein was cannulated under anesthesia by a 30-gauge needle and the needle was fixed by a cyanoacrylate adhesive. All experiments were carried out under room air.

All experimental protocols were reviewed by the Committee on the Ethics of Animal Experiments at School of Medicine, Keio University, and were carried out in accordance with Guidelines for Animal Experiments issued by the School of Medicine Keio University Experimental Animal Center and The Law (No. 105) and Notification (No. 6) issued by the Japanese Government. These guidelines meet the guidelines for animal handling issued by the National Institutes of Health (NIH).

Tumor Tissue Oxygen Tension Measurements

The tumor tissue oxygen tension was measured by the oxygen-dependent quenching of phosphorescence using Oxyspot phosphorimeter systems (Medical Systems Corp., Greenvale, NY). The skin over the tumor was carefully removed, and a glass coverslip was placed over the tumor. The skin on the back was also carefully removed and the back muscle was exposed followed by coverslip placement. Saline was injected under the coverslip to sustain moisture. The porphyrin probe (Oxygen Probe; Harvard Apparatus, Holliston, MA), 5,10,15,20-tetrakis(4-carboxylphenyl)porphinatoparadium, was provided as a lyophilized powder containing 9% probe, 80% bovine serum albumin (clinical grade, low fatty acid), 3% Trisma buffer, and 8% NaCl. It was dissolved in distilled water (pH 7.4) and administered through the tail vein (0.9 mL/kg). Approximately 5 min after probe administration, oxygen tension measurement was initiated. The light from the flash-lamp was filtered through an interference filter with 545-nm center wavelength and half-bandwidth of 45 nm. It was conducted through the light guide and focused on an approximately 8-mm-diameter area of the tumor tissue, approximately 4 mm from the tumor surface. The phosphorescence collected by the lens was introduced into the light guide and was filtered through a long pass filter at 645 nm, which was then led into the photomultiplier. The phosphorescence decay was fitted to a single exponential to determine the lifetime and oxygen partial pressure using the Stern–Volmer equation [22].

Measurements were made three times and averaged for each time point. Back skeletal muscle tissue oxygen tension was measured before and after tumor tissue oxygen tension measurements as control values. Tumor tissue oxygen tension was measured before (time 0), 1, 2, and 3 min after sample administration, and every 3 min thereafter until 45 min. Samples (saline: saline group, $n = 5$; HbV: HbV group, $n = 5$; metHbV: metHbV group, $n = 4$; lowP50HbV: lowP50HbV group, $n = 8$) were administered through the tail vein,12 mL/kg, in approximately 1 min.

Tumor Growth Measurements

Tumor growth measurements were made after sample administration followed by irradiation (saline: salinerad group, $n = 7$; HbV: HbVrad group, $n = 7$; metHbV: metHbVrad group, $n = 7$; lowP50HbV: lowP50HbVrad group, $n = 7$) or without irradiation (saline: salinenonrad group, $n = 5$; HbV: HbVnonrad group, $n = 4$). Single-dose irradiation (20 Gy) was delivered to the tumor-bearing

mice using a device designed for mouse bone marrow irradiation (Hitachi Medicotechnology, MBR-1520R-3, Hitachi, Japan). To irradiate only the tumor-bearing left hindlimb, a cage that shields the whole body except the tumor area from irradiation was used (Hitachi Medicotechnology, MBR-1520R-3). Power output of γ-irradiation was 150 Kv, 20 mAmp. A 0.5-mm aluminum filter was used to filtrate forward-scattered radiation. Before mouse placement, a dose measurement probe was placed inside the shield cage at the assigned tumor site, and test irradiation was done to determine the dose rate at the tumor location. Next, the probe was placed in an allocated position outside the cage, and test irradiation was done. From these two test dose rates, the dosage at the tumor site was automatically calculated in proportion to the dosage at the measurement probe. The dose rate at the tumor site was approximately 2.2 to 2.4 Gy per minute. It took approximately 8 min to complete 20-Gy irradiation using this device. Based on the measurements in tumor tissue oxygen tension following HbV administration, samples were administered approximately 10 min before the start of irradiation (salinerad, HbVrad, metHbVrad, lowP50HbVrad groups). Additionally, saline and HbV were administered without irradiation (salinenonrad, HbVnonrad groups). After sample administration with or without irradiation, the tail vein needle was removed, and the animals were allowed to recover from anesthesia. Tumors were measured using a venier caliper every 2 days up to 28 days after tumor implantation, after which point some animals started to show tumor-related distress. Estimated tumor weight was calculated as previously described [23]:

$$\text{Estimated tumor weight (mg)} = \text{longer tumor diameter (mm)} \times [\text{shorter tumor diameter (mm)}]^2/2.$$

Histological Studies and Hypoxia-Inducible Factor-1-alpha Analysis

In a separate group of animals, tumors were resected 20 min after intravenous administration of HbV ($n = 4$) or metHbV ($n = 4$). Half the tumor was fixed in 10% formalin for histology. The other half was immediately snap frozen in liquid nitrogen and stored at −80°C.

Paraffin sections were prepared from fixed tumor specimens and stained with hematoxylin and eosin for morphology. To locate HbV in tumor tissue, the human hemoglobin contained in the HbV was stained as previously described [8], with a rabbit polyclonal antibody against human hemoglobin (DAKO A/S, Copenhagen, Denmark) as the primary antibody. This antibody did not cross-react with mouse hemoglobin, which was evident from the fact that mouse RBCs were not stained. Reaction with the secondary antibody and color development were performed with the Ventana alkaline phosphatase RED detection kit using the Ventana NX system (Ventana Med. System, Inc., Tucson, AZ).

Western analysis for HIF1alpha protein was performed with the standard method. Briefly, cells were lysed with a denaturing buffer, and the lysate was centrifuged at 14,000 rpm for 15 min at 4°C. The supernatant was mixed with Laemmli buffer and applied to SDS-PAGE gels. The proteins were separated by 10% SDS-PAGE and then transferred to PVDF membrane for 90 min at 90 V using Novex Tris-Glycine system (Invitrogen, Carlsbad, CA). The primary antibody for HIF1alpha (clone 54; BD Bioscience, Franklin Lakes, NJ) was incubated with the blot overnight. The secondary anti-mouse IgG was incubated with the blots for 1 h. Bands were detected by enhanced chemiluminescence using Super Signal substrate (Pierce, Rockford, IL). Band densitometry was quantified using Image J (NIH, Bethesda, MA).

Data Analysis

Data are shown as mean ± standard deviation. Changes in tumor tissue oxygen tension and tumor growth measurements with or without irradiation were compared by analysis of variance followed by Scheffe's post-hoc test (StatView; Abacus, Berkeley, CA). Differences between groups at particular time points were compared by Mann–Whitney t-test (StatView; Abacus). Band densitometry was compared by Mann–Whitney t-test (StatView; Abacus). P values smaller than 5% were considered significant.

RESULTS

Sample administration and irradiation were well tolerated in all of the animals with no apparent changes in behavior or feeding.

Tumor Tissue Oxygen Tension Measurements

The tissue oxygen tension of back muscle before (saline: 14.4 ± 1.2; HbV: 14.2 ± 1.6; metHbV: 15.3 ± 1.2; lowP50HbV: 14.8 ± 1.2 (Torr)) and after (saline: 14.5 ± 1.1; HbV: 14.3 ± 1.4; metHbV: 15.3 ± 1.0; lowP50HbV: 14.6 ± 1.3 (Torr)) sample administration did not change significantly within or between groups. There were no significant differences in tumor tissue oxygen tension before sample administration (saline: 4.1 ± 1.1; HbV: 4.3 ± 0.8; metHbV: 4.3 ± 1.1; lowP50HbV: 4.3 ± 1.1 (Torr)). After sample administration, tumor tissue oxygen tension increased transiently in the HbV group during the observation period. Differences became significant from 15 to 30 min after sample administration in comparison to other groups. There was also a slight transient increase in the tumor tissue oxygen tension in the lowP50HbV group. Difference was significant between the saline group at 12 and 15 min after sample administration. Multiple comparisons using analysis of variance showed significant differences between HbV group curve and other groups. There was also a significant difference between lowP50HbV group curve and saline group curve (Fig. 1).

Tumor Growth Measurements

There were no significant differences in estimated tumor weight between groups at day 10 before sample administration, with or without irradiation (salinerad: 252 ± 27; HbVrad: 248 ± 38; metHbVrad: 239 ± 43; lowP50HbVrad: 248 ± 38; salinenonrad: 250 ± 33; HbVnonrad: 249 ± 38 (mg)). HbV administration without irradiation (HbVnonrad group) did not affect significant tumor growth delay in comparison to saline administration without irradiation (salinenonrad group). In both of these nonirradiated groups, tumor growth was significantly faster in comparison to any of the irradiated groups. Tumor growth delay after irradiation was marginally greater in the HbVrad group in comparison to other groups. Differences reached significance in the HbVrad group after irradiation in comparison to all other groups, from 16 to 28 days, except at day 24, at which point the difference was not significant between the metHbVrad group. Multiple comparisons

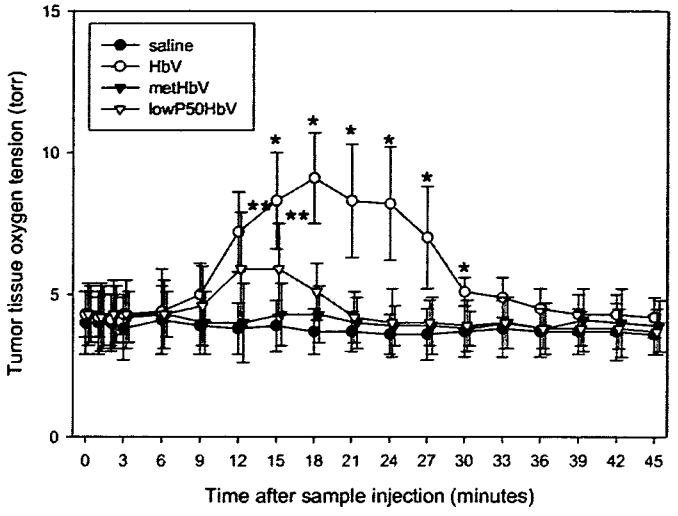

FIG. 1. Tumor tissue oxygen tension increased transiently in the HbV group. Differences became significant from 15 to 30 min after sample administration (*$P < 0.05$ *versus* all other groups, Mann–Whitney *t*-test). There was also a transient increase in the tumor tissue oxygen tension in the lowP50HbV group. Difference was significant between the saline group at 12 and 15 min after sample administration (**$P < 0.05$ *versus* saline group, Mann–Whitney *t*-test). Multiple comparisons using analysis of variance showed significant differences between the curves of HbV group and other groups. There was also a significant difference between the curves of lowP50HbV group, and saline group.

using analysis of variance showed significant differences between HbVrad group curve and all other groups (Fig. 2).

On hematoxylin and eosin staining, the tumors at day 10 were morphologically composed primarily of tumor cells, and tumor vessels, with very little extracellular matrix. Human hemoglobin staining revealed the presence of stained material not only within the tumor vessel (Fig. 3A) but also in the extracellular matrix (Fig. 3B), which were presumably extravasated HbV. On Western blot analysis, HIF1alpha level was significantly decreased in the HbV group in comparison to the metHbV group (Fig. 4).

DISCUSSION

One of the primary causes of tumor resistance to irradiation may be tumor tissue hypoxia. Although still far from conclusive in the clinic, this notion is generally accepted [24]. *In vitro* studies show that the presence of oxygen increases the cytotoxicity of irradiation, resulting in roughly a 3-fold difference in radiosensitivity between hypoxic and aerobic cells [25, 26]. This phenomenon is widely attributed to the oxygen's ability to chemically modify radiation-induced DNA damage, creating adducts that are not repaired by cells.

A correlation between tumor tissue oxygen tension status and therapeutic response after treatment with irradiation or chemotherapeutic agents has been observed in many preclinical studies. There is also accumulating clinical evidence that therapeutically significant tissue hypoxia frequently exists in human tumors. As a result, there has been a longstanding active research into novel methods of improving tumor tissue oxygenation, targeting hypoxic tumor cells, and/or modulating the effect hypoxia has on how tumors respond to treatment. Several methods of overcoming tumor tissue hypoxia are currently under investigation. These include hyperbaric oxygen, hyperthermia, and the use of potential radiosensitizers such as nitroimidazole-based substances, and pentoxifylline [27]. Artificial oxygen carriers, such as perfluorochemicals, and modified hemoglobins have also been evaluated for this purpose in several preclinical studies [28–34]. We have previously reported the effect of a totally synthetic-heme-based artificial oxygen carrier in oxygenating tumor tissue [35]. To our knowledge, tumor oxygenation using a liposome-type artificial oxygen carrier has not been closely tested.

The dose of HbV administered in this study, 12 mL/kg, is rather high in the context of a therapeutic drug. But since HbV is being developed primarily as a transfusion alternative, it should be possible to administer this dosage without complications in order for HbV to be clinically applicable. No adverse effects directly attributable to material administration were apparent with any of the administered samples. Oxygen tension of back muscle tissue did not change significantly with

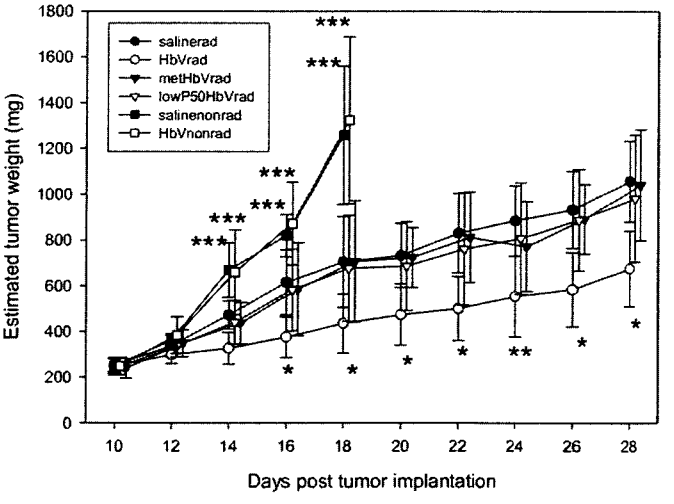

FIG. 2. Sample administration, saline, HbV, metHbV, lowP50HbV, with irradiation (salinerad, HbVrad, metHbVrad, lowP50HbVrad, groups respectively) or without irradiation (salinenonrad, HbVnonrad groups) were carried out on day 10. In the salinenonrad and HbVnonrad groups, tumor growth was significantly faster in comparison to any of the irradiated groups (***$P < 0.05$ *versus* groups that received irradiation, Mann–Whitney *t*-test). Tumor growth delay after irradiation was significantly increased in the HbVrad group in comparison to other groups (*$P < 0.05$ *versus* all other groups, Mann–Whitney *t*-test), except at day 24, at which point the difference was not significant between the metHbVrad group (**$P < 0.05$ *versus* all other groups except metHbV group, Mann–Whitney *t*-test). Multiple comparisons using analysis of variance showed a significant difference in the growth curves between HbVrad group, and all other groups.

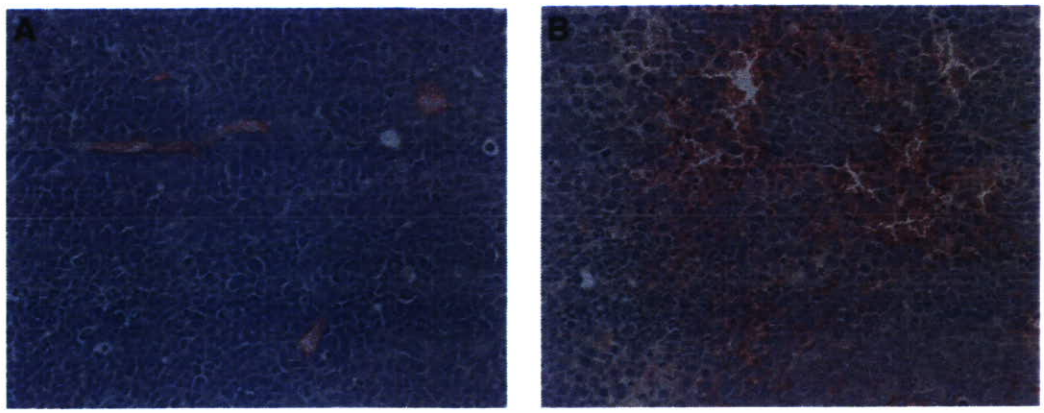

FIG. 3. Human hemoglobin staining could be seen not only within the tumor vessels (A) but also in the extracellular matrix (B) (human hemoglobin staining, ×20).

sample administration, but the measurements were made before and after the completion of tumor tissue oxygen tension measurements primarily to verify the integrity of light guide and lens. Therefore, a transient rise in muscle tissue oxygen tension as well as other normal tissues, possibly leading to toxicity, cannot be denied. Further studies are needed in this area.

In the present study, systemic administration of HbV transiently reduced tumor hypoxia, and moderately augmented tumor growth delay in response to irradiation in comparison to groups administered saline, metHbV, or lowP50HbV. HIF1alpha is a transcription factor activated by hypoxia, controlling many pathways in response to hypoxia in both normal and tumor cells. In the present study, tumor HIF1alpha protein level was significantly decreased at 20 min after HbV administration compared with metHbV administration. These results correlatively suggest that HbV augmented tumor growth delay following irradiation, at least in part, by affecting tumor tissue oxygen tension. However, the growth delay in the HbV group, although statistically significant, was marginal. A study using different irradiation dosages to determine TCD50 is necessary to further verify this effect. The involvement of other mechanisms is also possible. In the present study, metHbV administration did not have a significant effect on tumor tissue oxygen tension or irradiation response. Nevertheless, the effect of heme itself needs further investigation, because the heme within HbV could be the primary source of oxygen radical species formation following irradiation rather than the oxygen it delivers. It is also known that

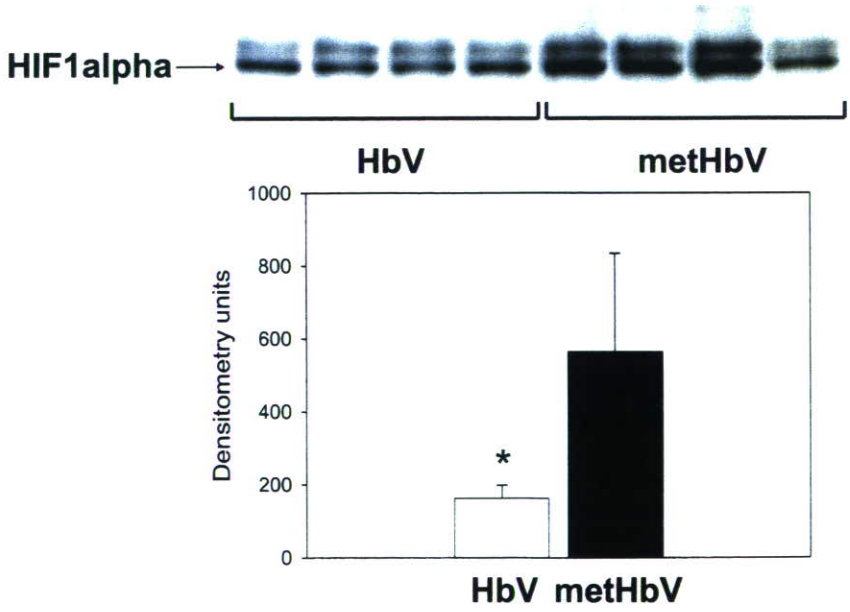

FIG. 4. HIF1alpha level was significantly decreased in the HbV group in comparison to the metHbV group. *P = 0.021 Mann–Whitney U-Test.

changes in HIF1alpha level itself modifies irradiation response, but both radiosensitization and radioprotection by changes in HIF1alpha level have been observed [36]. Further studies, including measurements at longer time points and with administration of other samples, are required to find out if the change in HIF1alpha level, with respect to or irrespective of change in tissue oxygen tension, is involved in this particular animal model.

The timing of tumor tissue oxygen tension elevation after artificial oxygen carrier administration differs among previous reports from approximately 4 min to 2 h [9, 28–35]. We do not have a clear answer as to why the increase in tumor tissue oxygen tension was transient in the present study. If the increase in tumor tissue oxygen tension was due to circulating HbV, the effect should have appeared over a longer duration because HbV is known to have a circulating half-life of approximately 48 h [37]. Therefore, we speculated that the increase in tumor tissue oxygen tension may have been affected primarily by extravasated HbV rather than circulating HbV and was hence transient. Tumor vessels are known to be morphologically heterogeneous and has highly permeable sites in comparison to normal vessels. Liposomes ranging in diameter from approximately 100 to 400 nm have been shown to extravasate into the tumor extracellular matrix presumably through these sites [38, 39]. In the present study, human hemoglobin staining revealed the presence of stained material not only within the tumor vasculature but also in the extracellular matrix. We know from previous experiments that hemoglobin is encapsulated within HbV until it is metabolized, which does not occur in this timeframe of 20 min after systemic administration [40]. So we consider that these were extravasated HbV. Lewis lung carcinoma used in this study formed tumors composed primarily of tumor cells and tumor vessels, with very little extracellular matrix. Because of this, the extravasated HbV mostly existed in the vicinity of tumor cells, and hence, may have modulated the tumor response to irradiation. Obviously these results may not be directly applicable to tumors encountered in the clinic, which contain significantly greater amounts of extracellular matrix.

Oxyspot used in this study only measures tissue oxygen tension close to the tissue surface. But since the Lewis lung carcinoma cell line used in this study formed a histologically homogeneous tumor composed primarily from tumor cells and vessels, with little extracellular matrix, we assume that the measurements made in this study sufficiently reflected tissue oxygen tension changes within the whole tumor. To this end, Lewis lung carcinoma line was suitable for this particular study, but its clinical relevance may be limited.

It has been reported that increase in hemoglobin affinity is beneficial for oxygen delivery to normal tissue particularly when oxygen supply is severely compromised [41, 42]. In the present study, there was only a minimal transient increase in tumor tissue oxygen tension after lowP50HbV administration, and benefit was not so apparent. Physiology of oxygen extraction may have been different between different tissues or tumor lines. Blood flow in tumor vessels is known to be highly variable, and regulatory mechanisms may not have functioned as in normal tissue. P_{50} of 8 Torr in lowP50HbV used in this study may have been too low for significant oxygen release in this particular model. Additionally, in the present study, the increase in tumor tissue oxygen tension may have been due to extravasated rather than circulating HbV, in which case the findings from previous studies which examine materials with low P_{50} supplying oxygen from within the circulation may not be directly applicable. Further studies are needed to find out if optimization of P_{50} significantly contributes to oxygenating tumor tissue.

Many types of liposomes are currently being developed to improve selective drug delivery to tumor tissue. HbV used in this study was developed as a transfusion alternative, but it may be possible to increase relative tumor distribution and further optimize HbV's irradiation augmentation effect by modifying its liposomal components as well as its P_{50}. These improvements may lead to similar or better outcome, with less dosage. The timing of irradiation also needs further study, including the use of fractionation.

ACKNOWLEDGMENTS

We thank Mr. Hitoshi Abe, Department of Pathology, School of Medicine, Keio University, for expertise in immunohistochemistry.

REFERENCES

1. Kobayashi K, Tsuchida E, Horinouchi H, eds. Artificial Oxygen Carrier: Its Front Line, Keio University International Symposia for Life Sciences and Medicine. Vol. 12, Springer-Verlag, 2005.
2. Chang TM. Hemoglobin based red blood cells substitutes. Artif Organs 2004;28:789.
3. Buehler PW, Alayash AI. Toxicities of hemoglobin solutions. in search of in-vitro and in-vivo model systems. Transfusion 2004; 44:1516.
4. Djordjevich L, Mayoral J, Miller IF, et al. Cardiorespiratory effects of exchanging transfusions with synthetic erythrocytes in rats. Crit Care Med 1987;15:318.
5. Awasthi VD, Garcia D, Klipper R, et al. Neutral and anionic liposome-encapsulated hemoglobin: effect of postinserted poly-(ethylene glycol)-distearoylphosphatidylethanolamine on distribution and circulation kinetics. J Pharmacol Exp Ther 2004; 309:241.
6. D'Agnillo F, Alayash AI. Redox cycling of diaspirin cross-linked hemoglobin induces G2/M arrest and apoptosis in cultured endothelial cells. Blood 2001;98:3315.
7. Sakai H, Hara H, Yuasa M, et al. Molecular dimensions of Hb-based O(2) carriers determine constriction of resistance arteries and hypertension. Am J Physiol Heart Circ Physiol 2000; 279:H908.

8. Sakai H, Horinouchi H, Yamamoto M, et al. Acute 40 percent exchange-transfusion with hemoglobin-vesicles (HbV) suspended in recombinant human serum albumin solution: Degradation of HbV and erythropoiesis in a rat spleen for 2 weeks. Transfusion 2006;46:339.
9. Sakai H, Horinouchi H, Tomiyama K, et al. Hemoglobin-vesicles as oxygen carriers: Influence on phagocytic activity and histopathological changes in reticuloendothelial system. Am J Pathol 2001;159:1079.
10. Sakai H, Masada Y, Horinouchi H, et al. Physiological capacity of the reticuloendothelial system for the degradation of hemoglobin vesicles (artificial oxygen carriers) after massive intravenous doses by daily repeated infusions for 14 days. J Pharmacol Exp Ther 2004;311:874.
11. Izumi Y, Sakai H, Hamada K, et al. Physiologic responses to exchange transfusion with hemoglobin vesicles as an artificial oxygen carrier in anesthetized rats: Changes in mean arterial pressure and renal cortical tissue oxygen tension. Crit Care Med 1996;24:1869.
12. Izumi Y, Sakai H, Kose T, et al. Evaluation of the capabilities of a hemoglobin vesicle as an artificial oxygen carrier in a rat exchange transfusion model. ASAIO J 1997;43:289.
13. Sakai H, Takeoka S, Wettstein R, et al. Systemic and microvascular responses to the hemorrhagic shock and resuscitation with Hb-vesicles. Am J Physiol Heart Circ Physiol 2002;283: H1191.
14. Sakai H, Masada Y, Horinouchi H, et al. Hemoglobin-vesicles suspended in recombinant human serum albumin for resuscitation from hemorrhagic shock in anesthetized rats. Crit Care Med 2004;32:539.
15. Yoshizu A, Izumi Y, Park S, et al. Hemorrhagic shock resuscitation with an artificial oxygen carrier, hemoglobin vesicle, maintains intestinal perfusion and suppresses the increase in plasma tumor necrosis factor-alpha. ASAIO J 2004;50:458.
16. Contaldo C, Plock J, Sakai H, et al. New generation of hemoglobin-based oxygen carriers evaluated for oxygenation of critically ischemic hamster flap tissue. Crit Care Med 2005;33:806.
17. Nozue M, Lee I, Manning JM, et al. Oxygenation in tumors by modified hemoglobins. J Surg Oncol 1996;62:109.
18. Takeoka S, Ohgushi T, Terase K, et al. Layer-controlled hemoglobin vesicles by interaction of hemoglobin with a phospholipid assembly. Langmuir 1996;12:1755.
19. Sakai H, Takeoka S, Park SI, et al. Surface-modification of hemoglobin vesicles with polyethyleneglycol and effects on aggregation, viscosity, and blood flow during 90%-exchange transfusion in anesthetized rats. Bioconjug Chem 1997;8:15.
20. Sakai H, Yusua M, Onuma H, et al. Synthesis and physicochemical characterization of a series of hemoglobin-based oxygen carriers: Objective comparison between cellular and acelluar types. Bioconjug Chem 2000;11:56.
21. Maeda N, Imaizumi K, Kon K, et al. A kinetic study on functional impairment of nitric oxide-exposed rat erythrocytes. Environ Health Perspect 1987;73:171.
22. Wilson DF, Cerniglia GJ. Localization of tumors and evaluation of their state of oxygenation by phosphorescence imaging. Cancer Res 1992;52:3988.
23. Ishikawa Y, Kubota T, Otani Y, et al. Dihydropyrimidine dehydrogenase activity and messenger RNA level may be related to the antitumor effect of 5-fluorouracil on human tumor xenografts in nude mice. Clin Cancer Res 1999;5:883.
24. Moeller BJ, Richardson RA, Dewhirst MW. Hypoxia and radiotherapy: Opportunities for improved outcomes in cancer treatment. Cancer Metastasis Rev 2007;26:241.
25. Gray LH, Conger AD, Ebert M, et al. The concentration of oxygen dissolved in tissues at the time of irradiation as a factor in radiotherapy. Br J Radiol 1953;26:638.
26. Deschner EE, Gray LH. Influence of oxygen tension on x-ray-induced chromosomal damage in Ehrlich ascites tumor cells irradiated in vitro and in vivo. Radiat Res 1959;11:115.
27. Lee I, Kim JH, Levitt SH, et al. Increases in tumor response by pentoxifylline alone or in combination with nicotinamide. Int J Radiat Oncol Biol Phys 1992;22:425.
28. Teicher BA, Herman TS, Hopkins RE, et al. Effect of oxygen level on the enhancement of tumor response to radiation by perfluorochemical emulsions or a bovine hemoglobin preparation. Int J Radiat Oncol Biol Phys 1991;21:969.
29. Teicher BA, Holden SA, Ara G, et al. Effect of a bovine hemoglobin preparation (SBHS) on the response of two murine solid tumors to radiation therapy or chemotherapeutic alkylating agents. Biomater Artif Cells Immob Biotechnol 1992;20:657.
30. Teicher BA, Herman TS, Menon K. Enhancement of fractionated radiation therapy by an experimental concentrated perflubron emulsion (Oxygent) in the Lewis lung carcinoma. Biomater Artif Cells Immob Biotechnol 1992;20:899.
31. Teicher BA, Dupuis NP, Robinson MF, et al. Reduced oxygenation in a rat mammary carcinoma post-radiation and reoxygenation with a perflubron emulsion/carbogen breathing. In Vivo 1994;8:125.
32. Teicher BA. An overview on oxygen carriers in cancer therapy. Artif Cells Blood Substit Immobil Biotechnol 1995;23:395.
33. Robinson MF, Dupuis NP, Kusumoto T, et al. Increased tumor oxygenation and radiation sensitivity in two rat tumors by a hemoglobin-based, oxygen-carrying preparation. Artif Cells Blood Substit Immobil Biotechnol 1995;23:431.
34. Linberg R, Conover CD, Shum KL, et al. Increased tissue oxygenation and enhanced radiation sensitivity of solid tumors in rodents following polyethylene glycol conjugated bovine hemoglobin administration. In Vivo 1998;12:167.
35. Kobayashi K, Komatsu T, Iwamaru A, et al. Oxygenation of hypoxic region in solid tumor by administration of human serum albumin incorporating synthetic hemes. J. Biomed Mater Res A 2003;64:48.
36. Moeller BJ, Dewhirst MW. HIF-1 and tumour radiosensitivity. Br J Cancer 2006;95:1.
37. Sou K, Klipper R, Goins B, et al. Circulation kinetics and organ distribution of Hb-vesicles developed as a red blood cell substitute. J Pharmacol Exp Ther 2005;312:702.
38. Yuan F, Dellian M, Fukumura D, et al. Vascular permeability in a human tumor xenograft: Molecular size dependence and cutoff size. Cancer Res 1995;55:3752.
39. Yuan F, Leunig M, Huang SK, et al. Microvascular permeability and interstitial penetration of sterically stabilized (stealth) liposomes in a human tumor xenograft. Cancer Res 1994;54: 3352.
40. Takeoka S, Teramura Y, Atoji T, et al. Effect of Hb-encapsulation with vesicles on H_2O_2 reaction and lipid peroxidation. Bioconjug Chem 2002;13:1302.
41. Stein JC, Ellsworth ML. Capillary oxygen transport during severe hypoxia: Role of hemoglobin oxygen affinity. J Appl Physiol 1993;75:1601.
42. Sakai H, Cabrales P, Tsai AG, et al. Oxygen release from low and normal P_{50} Hb vesicles in transiently occluded arterioles of the hamster window model. Am J Physiol Heart Circ Physiol 2005;288:H2897.

ISSN 0954-6820 Vol. 263 No. 1 January 2008
www.blackwellpublishing.com/jim
www.jim.se

Journal of INTERNAL MEDICINE

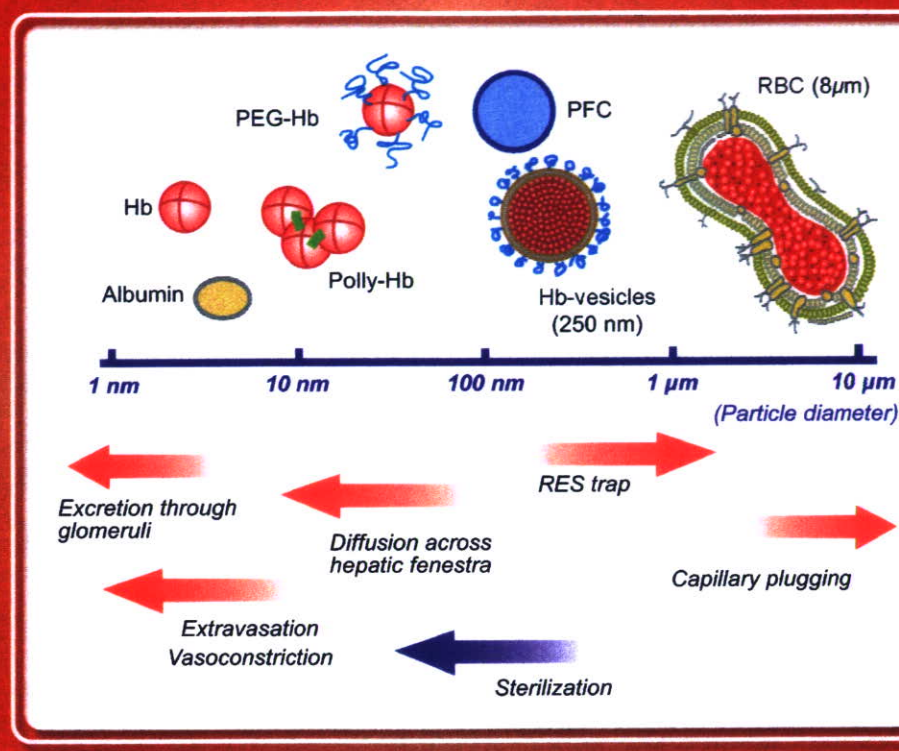

Blackwell Publishing

Review | Journal of INTERNAL MEDICINE

doi: 10.1111/j.1365-2796.2007.01893.x

Haemoglobin-vesicles as artificial oxygen carriers: present situation and future visions

● H. Sakai[1], K. Sou[1], H. Horinouchi[2], K. Kobayashi[2] & E. Tsuchida[1]

From the [1]Oxygen Infusion Project, Advanced Research Institute for Science and Engineering, Waseda University; and [2]Department of General Thoracic Surgery, School of Medicine, Keio University; Tokyo, Japan

Abstract. Sakai H, Sou K, Horinouchi H, Kobayashi K, Tsuchida E (Research Institute for Science and Engineering, Waseda University; and School of Medicine, Keio University; Tokyo, Japan). Haemoglobin-vesicles as artificial oxygen carriers: present situation and future visions (Review). *J Intern Med* 2008; **263**: 4–15.

During the long history of development of haemoglobin (Hb)-based O_2 carriers (HBOCs), many side effects of Hb molecules have become apparent. They imply the physiological importance of the cellular structure of red blood cells. Hb-vesicles (HbV) are artificial O_2 carriers that encapsulate concentrated Hb solution with a thin lipid membrane. We have overcome the intrinsic issues of the suspension of HbV as a molecular assembly, such as stability for storage and in blood circulation, blood compatibility and prompt degradation in the reticuloendothelial system. Animal tests clarified the efficacy of HbV as a transfusion alternative and the possibility for other clinical applications. The results of ongoing HbV research make us confident in advancing further development of HbV, with the expectation of its eventual realization.

Keywords: artificial oxygen carrier, biocompatibility, liposome, nanotechnology, polyethylene glycol.

Introduction

Since the discovery of blood type antigen by Landsteinter in 1900, allogeneic blood transfusion has developed into a routine clinical practice; it has contributed to human health and welfare. Infectious diseases such as hepatitis and HIV have become widespread social problems, but a strict virus test by nucleic acid amplification test (NAT) is extremely effective to detect trace presences of a virus to minimize infection (although it is available mainly in a few developed countries). Even so, NAT poses problems such as detection limits during a window period and limited species of viruses for testing. Emergence of new viruses (such as West Nile virus, avian influenza and Ebola) and a new type of pathogen, prions, also threaten humans throughout the world. The preservation period of donated red blood cells (RBCs) is limited to 3 weeks in Japan. Immunological responses (such as anaphylaxis and graft-versus-host disease), and contingencies of blood type incompatibility further limit the utility of blood products. To obviate or minimize homologous transfusion, the transfusion trigger has been reconsidered, and roughly reduced from 10 to 6–8 g dL^{-1}. Bloodless surgery and preoperational enhancement of erythropoiesis for storing autologous blood have become common. However, these epoch-making treatments are not always practical for all patients. Some developed countries with ageing populations are confronting a decreasing number of young donors and an increasing number of aged recipients. Prohibition of blood donation from people who have travelled certain countries during a specific period also exacerbates the blood shortage in Japan. On the other hand, in some developing countries, establishment of a safe blood donation system is difficult. Under such circumstances, research of blood substitutes has gathered great attention and has been developed worldwide [1–4]. In Japan, for example, the government has given strong support to development of blood

substitutes in the wake of two tragedies: infection, by AIDS, of haemophiliac patients who had received nonpasteurized plasma products and the Great Hanshin Earthquake disaster. The requisites for artificial oxygen carriers that we develop should be not only effectiveness for tissue oxygenation, but also the following:

1 No blood type antigen and no infection (no pathogens);
2 Stability for long-term storage (e.g. over 2 years) at room temperature for stockpiling for any emergency;
3 Low toxicity and prompt metabolism, even after massive infusion;
4 Physichochemical properties that are adjustable to resemble those of human blood and
5 Reasonable production expense and cost performance.
Realization of such an artificial oxygen carrier will revolutionize transfusion medicine.

Physiological significance of cellular structure

Physicochemical measurements of O_2-releasing behaviours have revealed that the cellular structure of RBCs might not be effective for facilitating O_2 releasing in comparison with a homogeneous haemoglobin (Hb) solution [5–7]. However, nature has selected this cellular structure through evolution. The reasons for Hb encapsulation in RBCs are: (i) a decrease in the high colloidal osmotic pressure of Hb; (ii) prevention of the removal of Hb from blood circulation and (iii) preservation of the chemical environment in cells, such as the concentration of phosphates (2,3-diphosphoglyceric acid (DPG), ATP, etc.) and other electrolytes. Moreover, during the long history of the development of Hb-based O_2 carriers (HBOCs), many side effects of Hb molecules have become apparent, such as the dissociation of tetrameric Hb subunits into two dimers ($\alpha_2\beta_2 \rightarrow 2\alpha\beta$) that might induce renal toxicity, and entrapment of gaseous messenger molecules (NO and CO) inducing vasoconstriction, hypertension, reduced blood flow and tissue oxygenation at microcirculatory levels [8, 9], neurological disturbances, and the malfunctioning of oesophageal motor function [10]. These side effects of Hb molecules imply the importance of the cellular structure (Fig. 1).

Pioneering work of Hb encapsulation to mimic the cellular structure of RBCs was performed by Chang in 1957 [1], who prepared microcapsules (5 μm) made of nylon, collodion, etc. Toyoda in 1965 [11] and the Kambara-Kimoto group [12] also covered Hb solutions with gelatine, gum Arabic, silicone, etc. Nevertheless, it was shown to be extremely difficult to regulate the particle size that was appropriate for blood flow in the capillaries and to obtain sufficient biocompatibility. After Bangham and Horne reported in 1964 that phospholipids assemble to form vesicles in aqueous media, and that they encapsulate water-soluble materials in their inner aqueous interior [13], it seemed reasonable to use such vesicles for Hb encapsulation. Djordjevich and Miller in 1977 prepared liposome-encapsulated Hb (LEH) composed of phospholipids, cholesterol, fatty acids, etc. [14]. In the US, Naval Research Laboratories showed remarkable progress of LEH [15].

However, some intrinsic issues of encapsulated Hbs remained, mainly related to molecular assembly and particle dispersion. What we call Hb-vesicles (HbV) with high-efficiency production processes and their improved properties, were established by Tsuchida's group [16–18] based on technologies of molecular assembly and precise analysis of pharmacological and physiological aspects (Fig. 2). The salient characteristics of HbV are the following:

1 Human Hb is purified completely via pasteurization at 60 °C and ultrafiltration; no viruses exist [19–21];
2 A concentrated Hb solution, nearly 35 g dL^{-1}, is encapsulated with a thin bilayer membrane [16–18];
3 A new synthetic lipid is used to prevent platelet (PLT) activation [22, 23];
4 PEG-modification guarantees long-term storage over 2 years at room temperature, blood compatibility and extended circulation half-life [24–30];